



Synthesis, Characterization, Crystal Structure, and Hirshfeld Surface Analysis of (2Z)-3-(methylsulfanyl)-2,3-diphenylprop 2-enenitrile

A. C. Vinayaka, R. Manjunath, S. Madan Kumar, M. M. Abdoh, M. P. Sadashiva & N. K. Lokanath

To cite this article: A. C. Vinayaka, R. Manjunath, S. Madan Kumar, M. M. Abdoh, M. P. Sadashiva & N. K. Lokanath (2015) Synthesis, Characterization, Crystal Structure, and Hirshfeld Surface Analysis of (2Z)-3-(methylsulfanyl)-2,3-diphenylprop 2-enenitrile, *Molecular Crystals and Liquid Crystals*, 609:1, 140-154, DOI: [10.1080/15421406.2014.950456](https://doi.org/10.1080/15421406.2014.950456)

To link to this article: <http://dx.doi.org/10.1080/15421406.2014.950456>



Published online: 11 Apr 2015.



Submit your article to this journal [↗](#)



Article views: 63



View related articles [↗](#)



View Crossmark data [↗](#)

Synthesis, Characterization, Crystal Structure, and Hirshfeld Surface Analysis of (2Z)-3-(methylsulfanyl)-2,3- diphenylprop 2-enenitrile

A. C. VINAYAKA,¹ R. MANJUNATH,² S. MADAN KUMAR,³
M. M. ABDOH,⁴ M. P. SADASHIVA,¹ AND N. K. LOKANATH^{3,*}

¹Department of Studies in Chemistry, University of Mysore, Mysore, India

²Department of Physics, SBRR Mahajana First Grade College, Mysore, India

³Department of Studies in Physics, University of Mysore, Mysore, India

⁴Department of Physics, Faculty of Science, AnNajah National University,
Nabtus West Bank, Palestinian Territories

The title compound, C₁₆H₁₃NS (3) was synthesized and characterized by ¹H nuclear magnetic resonance (NMR), mass spectra (MS), infrared (IR), thermogravimetric analysis, differential scanning calorimeter (DSC) and finally the structure is confirmed by single crystal X-ray diffraction method. The compound 3 crystallizes in the monoclinic crystal system and space group C2/c, with crystal parameters, a = 10.99364(4) Å, b = 12.3517(3) Å, c = 20.1045(6) Å, β = 103.082(3)°, Z = 8, and V = 2647.30(14) Å³. The structure of the compound reveals that the intermolecular interactions of the type C–H...π, C–H...N, and S...S. The packing diagram of the molecules in the unit cell exhibit three-dimensional architecture. In addition inter contacts involved in intermolecular interactions are quantified using Hirshfeld surfaces analysis.

Keywords Crystal structure; Hirshfeld surfaces; intermolecular interaction; ketene thioacetal

1. Introduction

Ketene thioacetals are key intermediates in wide variety of organic synthesis and have versatile synthetic intermediate properties [1]. They have been employed as precursors to aldehydes [2], ketones [3], carboxylic acids [4], and cyclopropanes [5], also they are used as substrates in Diels–Alder reactions [6] and as Michael acceptors [7]. In the synthesis of pyrrolizidine ring system ketene thioacetals acts as a cationic cyclization terminator [8], which results in heterocyclic products such as thiophenes [9] and indoles [10]. The products of heterocyclization compounds reveal pharmaceutical properties such as antipsychotic [11], antidepressive [12], antithrombotic [13], anti-inflammatory [14, 15], and they are important in the synthesis of the potent pancreatic lipase inhibitor, Panclin D [16]. Such

*Address correspondence to N. K. Lokanath, Department of Studies in Physics, University of Mysore 570006, Mysore, India. E-mail: lokanath@physics.uni-mysore.ac.in

Color versions of one or more of the figures in the article can be found online at www.tandfonline.com/gmcl.

organosulfur compounds, the presence of nonbonding interactions of the type S...S play a significant role in controlling the molecular conformation, packing of molecules in crystals and molecular recognition. Moreover, these interactions are interested in relation to the bioactivity of a variety of compounds containing sulfur atoms. Also these interactions can induce high electron dimensionality in many organic superconductors [17]. Recent trends in crystal engineering, the identification or design of molecular level building blocks (supramolecular synthons), through intermolecular interaction exhibits some degree of predictability [18]. In addition to chemical and biological applications, this compound is also used as synthetic intermediate in the enhancement of photovoltaic of a novel dye T18, for high efficiency dye sensitized solar cells [19]. With the background of above-mentioned important properties, herein we report the synthesis, characterization and crystal structure of (2Z)-3-(methylsulfanyl)-2,3-diphenylprop-2-enenitrile (**3**). The structure of the compound **3** was established with the results of ^1H NMR, MS, IR, thermogravimetric analysis (TGA), DSC, and finally confirmed by X-ray diffraction method. The intermolecular interaction of the title compound has been investigated using Hirshfeld surface computational method.

2. Experimental

2.1. Materials and Methods

^1H NMR spectra were recorded on a Bruker AMX-400. Infrared spectra were recorded on a Perkin Elmer spectrometer model spectrum two in OptKBr. Mass spectra were recorded using electrospray ionization (ESI) mass spectrometry. The C, H, and N analysis were performed using Elementar Vario EL III analyzer. TGA experiment was performed using instrument TGA Q50 and Differential Scanning Calorimetry using DSCQ200.

2.2. Procedure for the Preparation of

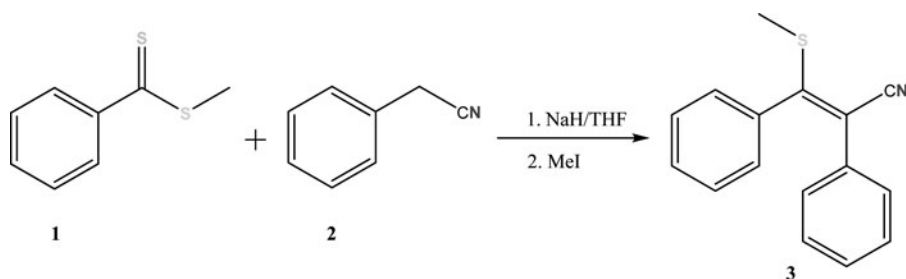
(2Z)-3-(methylsulfanyl)-2,3-diphenylprop-2-enenitrile (**3**)

A mixture of methyl benzenecarbodithioate (**1**, 0.002 mol) and phenylacetoneitrile (**2**, 0.002 mol) was added drop wise to the suspension of NaH (0.005 mol) in tetrahydrofuran at 0°C under stirring. The reaction mixture was stirred at room temperature for two hours and then added methyl iodide (0.0023 mol). Again the resulting mixture was stirred for 3 hr and the reaction was monitored by TLC. Cold water is added to the reaction mixture and the sample was extracted with ethyl acetate ($2 \times 10\text{ mL}$), washed with brine ($1 \times 10\text{ mL}$), and dried over anhydrous Na_2SO_4 . The solvent was evaporated under reduced pressure to give crude product **3**. Later, it was purified by column chromatography over silica gel (60–120 mesh) using hexane: ethyl acetate mixture in 9:1 ratio as eluent. The yield was 96% with melting point $140\text{--}143^\circ\text{C}$. The sample is crystallized using slow evaporation method (ethanol); red-colored single crystals were obtained. The reaction scheme for the synthesis of the title compound **3** is as shown in Scheme I.

3. Results and Discussion

3.1. FT-IR Spectral Analysis

The FT-IR spectrum of the crystal structure is shown in Fig. 1. The absorption peaks were found to be 2202 cm^{-1} ($-\text{CN}$), 1546.6 cm^{-1} ($\text{C}=\text{C}$), 1444.97 cm^{-1} , 748.57 cm^{-1} , and 695.4 cm^{-1} .



Scheme 1. Synthesis of compound (2Z)-3-(methylsulfanyl)-2,3-diphenylprop-2-enenitrile.

3.2. ^1H NMR Spectral Analysis

The ^1H NMR spectrum of compound **3** was shown in Fig. 2. ^1H NMR spectrum showed sharp singlet corresponds to three protons at δ 2.04 ppm due to S—CH₃. The ten aromatic protons resonated as multiplet in the region of δ 7.08–7.31 ppm.

3.3. LC-MS Analysis

The formation of the compound **3** is confirmed by LC-MS analysis in Fig. 3. The peak at m/z 252(M^++1) correspond to molecular ion peak of compound having mass 251.

3.4. Thermogravimetric Analysis

The descending green TGA thermal curve of 10 mg of (2Z)-3-(methylsulfanyl)-2,3-diphenylprop-2-enenitrile indicates that the compound decomposes in one stage on heating between 250 and 600°C. The blue curve has one peak and this confirms that there is only one distinct thermal event taking place in this experiment. There was no weight loss up to 120°C, which indicates the absence of moisture in the crystal. Between 120 and 285°C there is gradual decrease in the weight, shows the pyrolysis of small crystalline compound taking place by breaking of C—SMe, C=C, C-CN bond and two phenyl rings. Above 400°C only 4% of the residue was left out, which was due to charring of carbon.

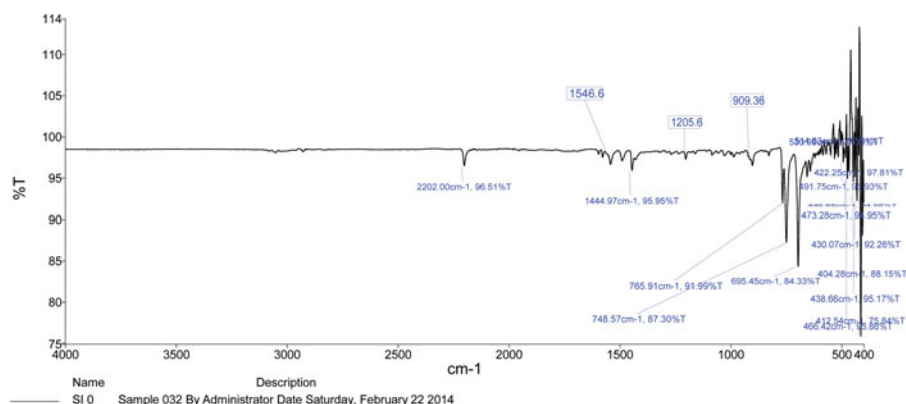


Figure 1. FT-IR spectra.

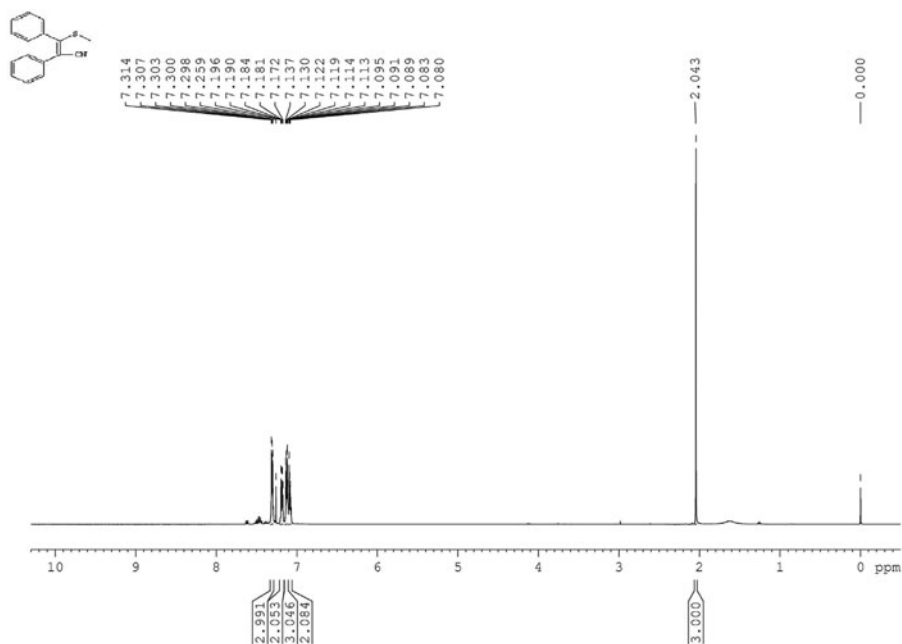


Figure 2. ¹H NMR spectra.

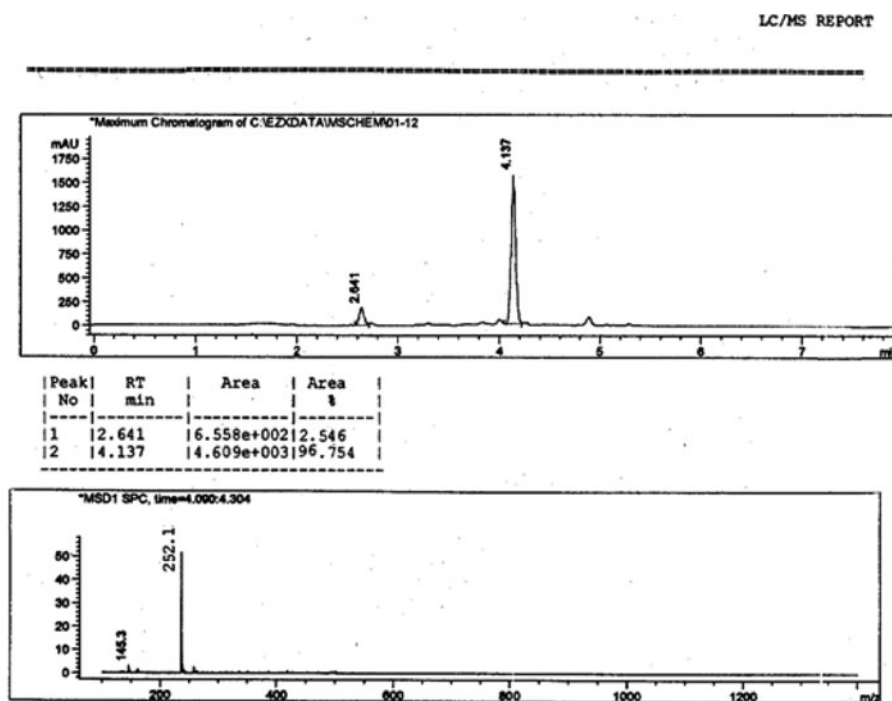


Figure 3. LC-MS spectra.

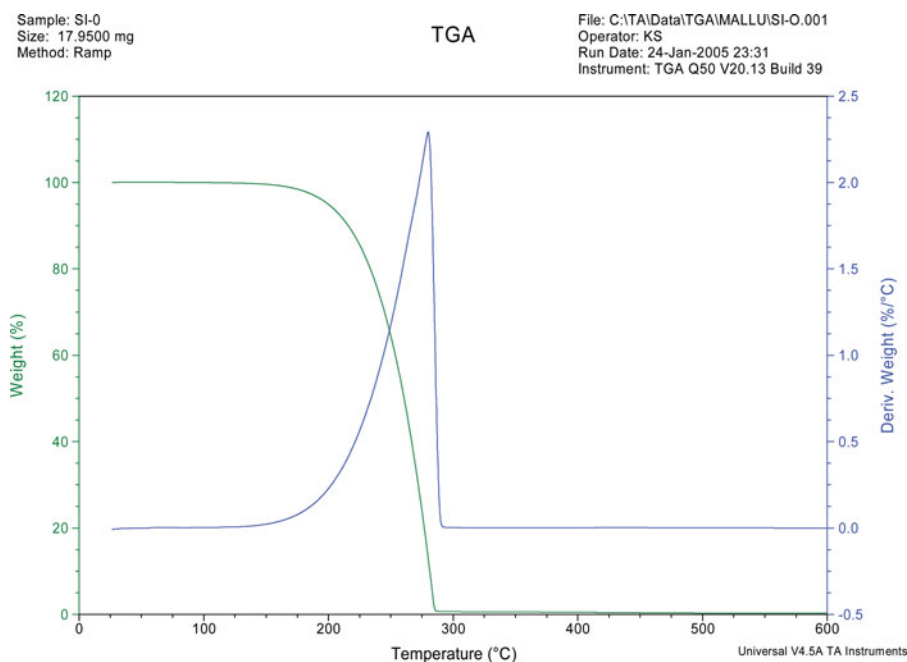


Figure 4. TGA thermogram of title compound.

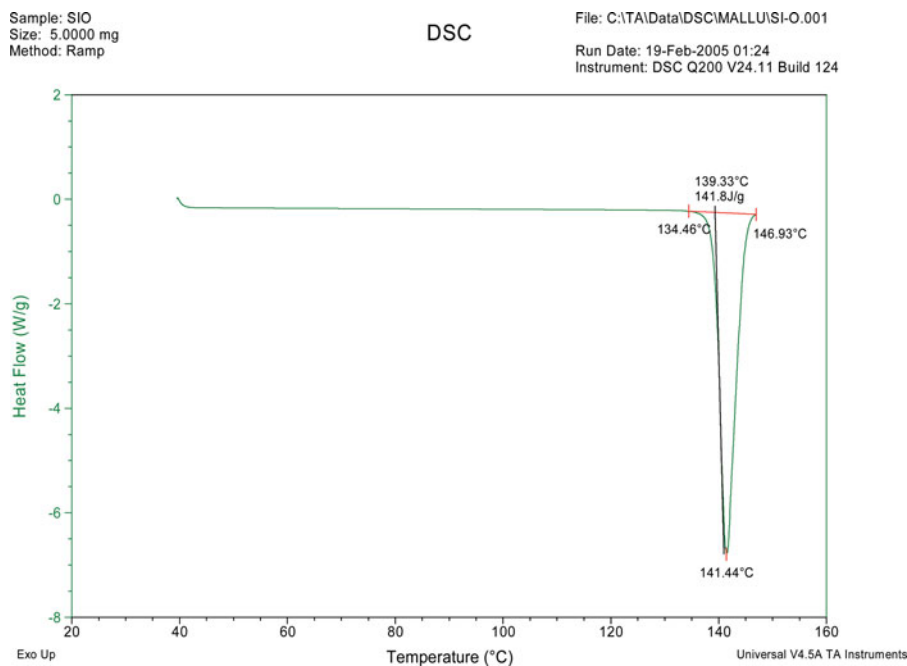


Figure 5. DSC thermogram of the title compound.

Table 1. Elemental analysis for C₁₆H₁₃NS

Element	Experimental (%)	Calculated (%)
Carbon	76.49	76.46
Nitrogen	5.54	5.57
Hydrogen	5.26	5.21

3.5. Differential Scanning Calorimetry

The DSC thermogram of the title compound is shown in Fig. 5. The thermogram of the (2Z)-3-(methylsulfanyl)-2,3-diphenylprop-2-enenitrile yields an endothermic peak at 141 °C (Fig. 4).

3.6. Elemental Analysis

In order to confirm the chemical composition of the synthesized compound carbon (C), hydrogen (H), and nitrogen (N) analysis was carried out. The experimental and calculated percentages of C, H, and N were given in Table 1. The differences between experimental and calculated percentages of C, H, and N were very close to each other and within the experimental errors. This confirms the formation of the product in the stoichiometric proportion.

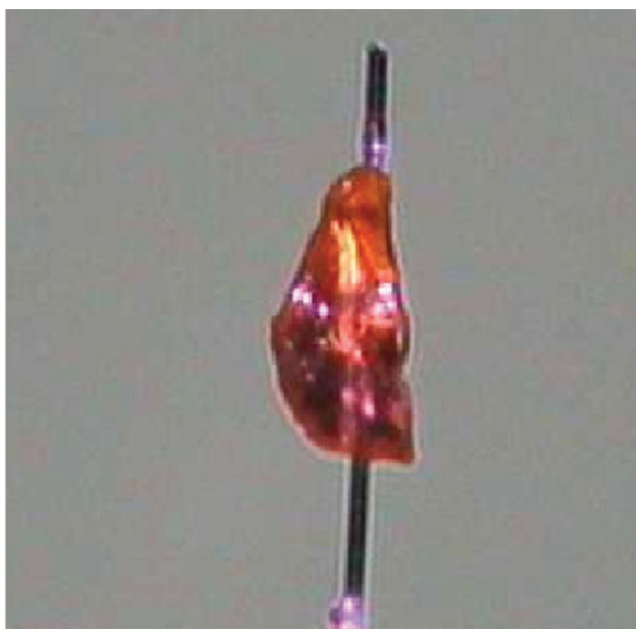


Figure 6. Crystal of the title compound. The crystal has approximate dimensions of 0.09 × 0.12 × 0.23 mm.

Table 2. Crystal data and structure refinement parameters of the title compound^a

CCDC deposition number	859959*
Empirical formula	C ₁₆ H ₁₃ N S
Formula weight	251.34
Temperature	296(2) K
Wavelength	1.5418 Å
Crystal system	monoclinic
Space group	<i>C</i> 2/ <i>c</i>
Unit cell dimensions	<i>a</i> = 10.9364(4) Å <i>b</i> = 12.3517(3) Å <i>c</i> = 20.1045(6) Å β = 103.082(3) °
Volume	2645.30(14) Å ³
<i>Z</i>	8
Calculated density	1.262 Mg/m ³
Absorption coefficient	1.993 mm ⁻¹
<i>F</i> ₍₀₀₀₎	1056
Crystal size	0.23 × 0.12 × 0.09 mm
Theta range for data collection	4.52° to 66.56°
Limiting indices	−12 < = <i>h</i> < = 12, −14 < = <i>k</i> < = 14, −23 < = <i>l</i> < = 23
Unique reflections	2585
Refinement method	Full-matrix least-squares on <i>F</i> ²
Data/restraints/parameters	2585/0/165
Goodness-of-fit on <i>F</i> ²	1.065
Final <i>R</i> indices [<i>I</i> > 2σ(<i>I</i>)]	<i>R</i> ₁ = 0.0372, <i>wR</i> ₂ = 0.0975
Largest diff. peak and hole	0.233 and −0.283 e.Å ⁻³

^aCCDC 859959 contains the supplementary crystallographic data for this paper. These data can be obtained free of charge via www.ccdc.cam.ac.uk/conts/retrieving.html (or from the Cambridge Crystallographic Data Centre, 12 Union Road, Cambridge CB2 1EZ, UK; fax: +44(0)1223-336033; email: deposit@ccdc.cam.ac.uk)

Table 3. Selected bond lengths (°)

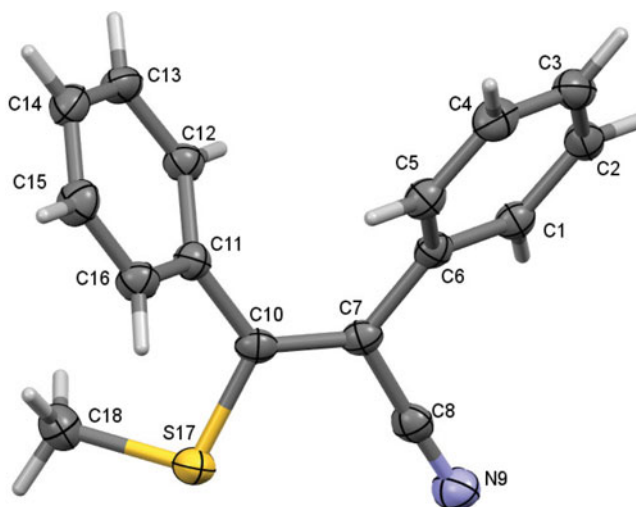
Atoms	Length	Atoms	Length
C1-C2	1.383(2)	C8-N9	1.149(2)
C1-C6	1.399(2)	C10-C11	1.490(2)
C2-C3	1.383(3)	C10-S17	1.7556(2)
C3-C4	1.386(3)	C11-C12	1.389(2)
C4-C5	1.386(3)	C11-C16	1.393(2)
C5-C6	1.399(2)	C12-C13	1.390(2)
C6-C7	1.485(2)	C13-C14	1.382(3)
C7-C10	1.360(2)	C14-C15	1.383(3)
C7-C8	1.446(2)	C15-C16	1.384(2)
S17-C18	1.7989(2)		

Table 4. Selected bond angles (°)

Atoms	Angle	Atoms	Angle
C2-C1-C6	121.16(16)	C7-C10-C11	123.68(15)
C1-C2-C3	119.81(17)	C7-C10-S17	118.31(13)
C2-C3-C4	119.75(17)	C11-C10-S17	117.95(12)
C3-C4-C5	120.86(17)	C12-C11-C16	119.72(16)
C4-C5-C6	119.91(16)	C12-C11-C10	120.60(15)
C5-C6-C1	118.50(15)	C16-C11-C10	119.64(14)
C5-C6-C7	122.17(15)	C11-C12-C13	119.65(16)
C1-C6-C7	119.29(14)	C14-C13-C12	120.28(16)
C10-C7-C8	117.82(15)	C13-C14-C15	120.26(16)
C10-C7-C6	127.67(15)	C14-C15-C16	119.79(17)
C8-C7-C6	114.50(14)	C15-C16-C11	120.26(16)
N9-C8-C7	177.6(2)	C10-S17-C18	103.47(8)

Table 5. Hydrogen bonding geometry (Å, °)

D-H...A	D-H	H...A	D...A	D-H...A	Symmetry code
C18-H18B...N9	0.96	2.61	3.458(3)	148	1/2-x, 3/2-y, 1-z

**Figure 7.** ORTEP view of the title molecule with atom numbering scheme. Displacement ellipsoids for non-hydrogen atoms are drawn at 50% probability level.

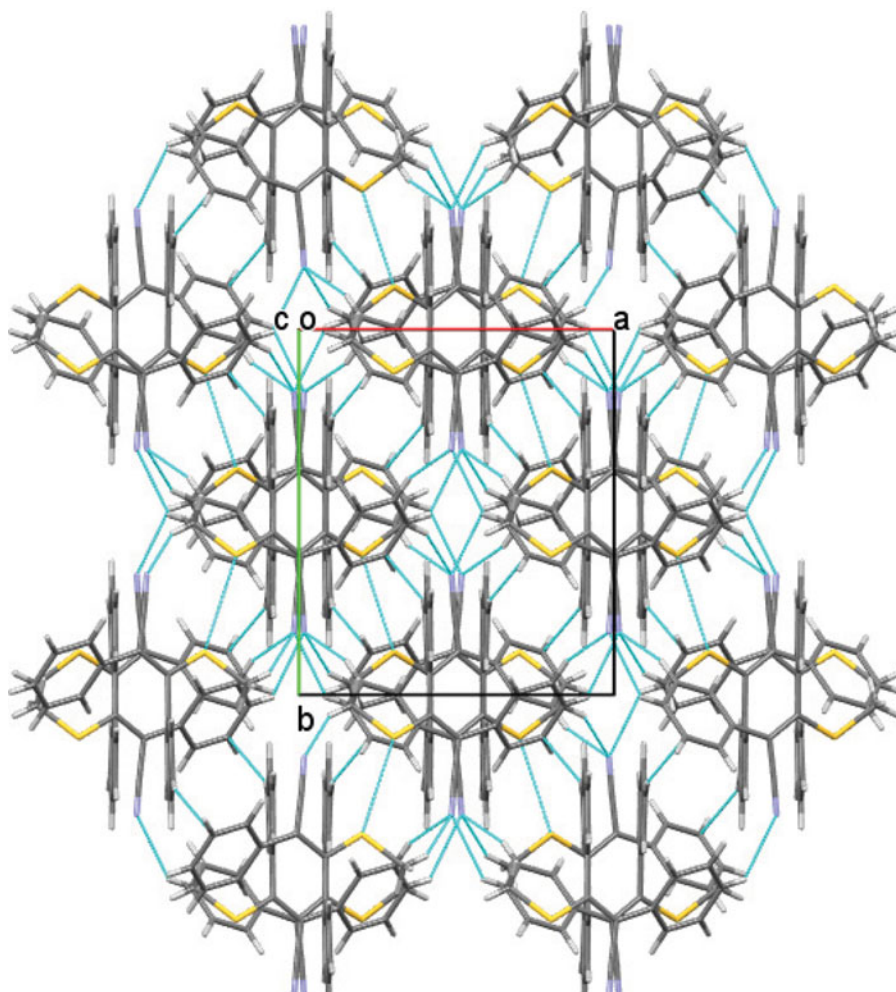


Figure 8. Packing of molecules when viewed down *c*-axis.

3.7. Single Crystal X-Ray Diffraction Method

A single crystal of the title compound **3** with dimension $0.09 \times 0.12 \times 0.23$ mm was chosen for X-ray diffraction study as shown in Fig. 6. Data collection and cell refinement were carried out using SuperNova diffractometer (Atlas CCD detector) with mirror multilayer optic monochromated Cu K_{α} radiation at 103 K. The crystal to detector distance is fixed at 50 mm. Five-twenty frames of data were collected. Each frame exposure time is set to 1 sec and also the scan width set to 10. The diffraction intensities were corrected for Lorentz and polarization factors. The numerical absorption corrections were applied to the program CrysAlisPro [20] using analytical method [21]. All the frames could be indexed using a primitive monoclinic lattice. The structure was solved by direct methods using SHELXS-97 [22]. All the non-hydrogen atoms were revealed in the first Fourier map itself. Full-matrix least squares refinement using SHELXL-97 [23] with isotropic temperature factors for all the atoms was done. Refinement of non-hydrogen atoms with anisotropic parameters was started at this stage. The hydrogen atoms were placed at chemically acceptable positions

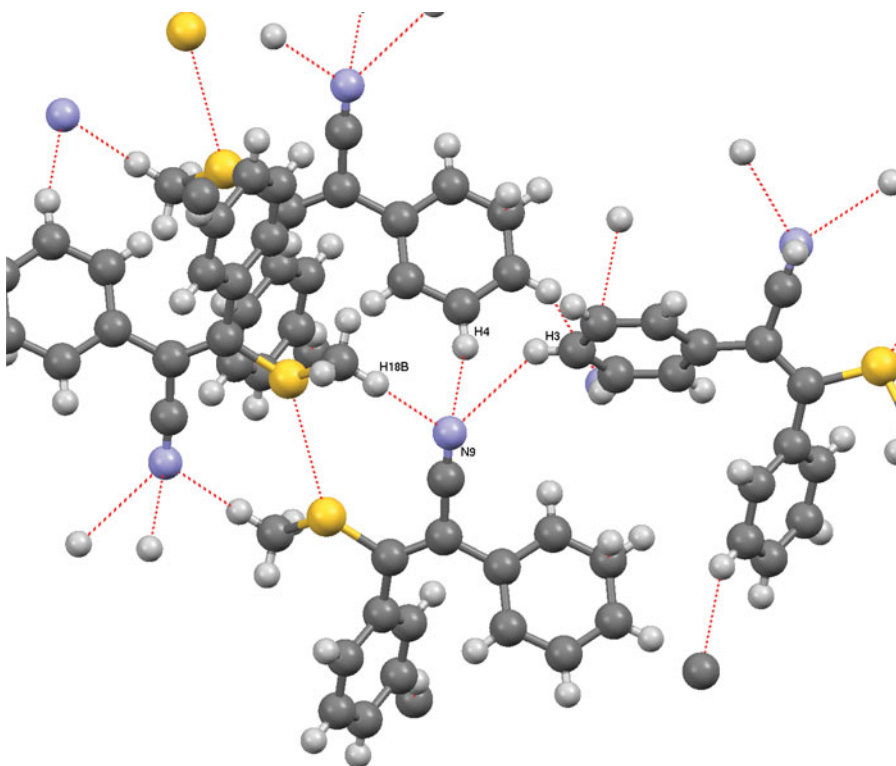


Figure 9. Trifurcated hydrogen bonding. Hydrogen bonding (dashed line) between atoms N9 to H18B, H3, and H4 are labeled.

and were allowed to ride on the parent atoms. About 165 parameters were refined with 2585 unique reflections which saturated the residuals to $R1 = 0.0372$ and $wR2 = 0.0975$. The ORTEP, intermolecular hydrogen bonding and packing diagrams were drawn using MERCURY [24]. The crystal data and refinement parameters are summarized in Table 2. Tables 3 and 4 list the selected bond distances and bond angles of non-hydrogen atoms, respectively. Hydrogen-bond geometry is given in Table 5.

The dihedral angle between the phenyl rings is $60.87(8)^\circ$, which is larger when compared to the similar structure of ethyl 2, 5-diphenylfuran-3-carboxylate [25]. The distortion in the bond angles are observed for C6–C7–C8, C6–C7–C10, and C7–C10–C11 atoms are $114.50(14)^\circ$, $127.67(14)^\circ$, and $123.68(14)^\circ$, respectively, suggests the steric hindrance caused by an electronic effect of the double bond between the atoms C7–C10 ($1.361(2) \text{ \AA}$)

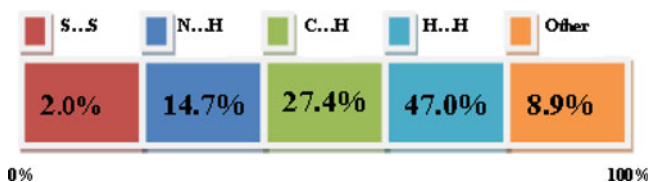


Figure 10. Hirshfeld surface. Percentage of various intermolecular contacts is contributed to the Hirshfeld surface.

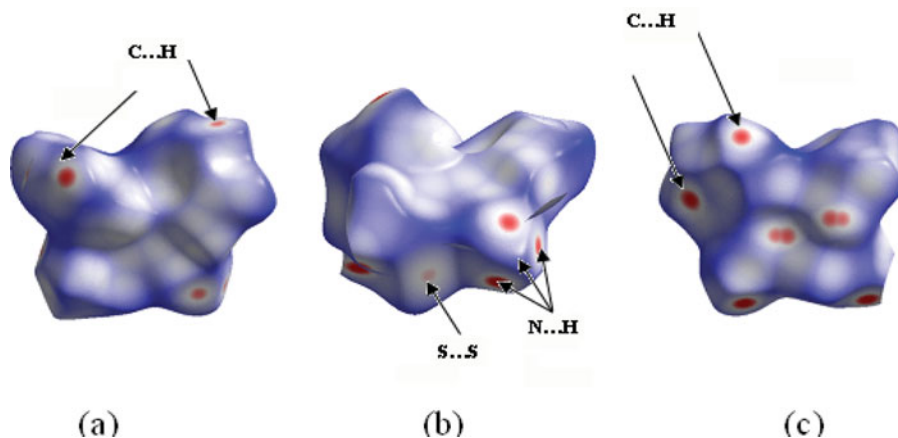


Figure 11. Dnorm mapped on Hirshfeld surface for visualizing the C...H, N...H, and S...S contacts of the compound **3** Hirshfeld surface.

linking four conjugated moiety. The bond angles of $117.82(15)^\circ$ and $118.32(12)^\circ$, for the atoms C8—C7—C10 and S17—C10—C7 confirms Z-configuration [26]. The N9—C8—C7 atoms adopt linearity, which is confirmed by the bond angle of $177.57(19)^\circ$. Figure 7 represents the ORTEP [27] diagram of the molecule with thermal ellipsoids drawn at 50% probability. The bond length of C7—C8 ($1.446(2)$ Å), is low compared to the bond length of C6—C7 ($1.486(2)$ Å) and C10—C11 ($1.490(2)$ Å), respectively indicating the delocalization

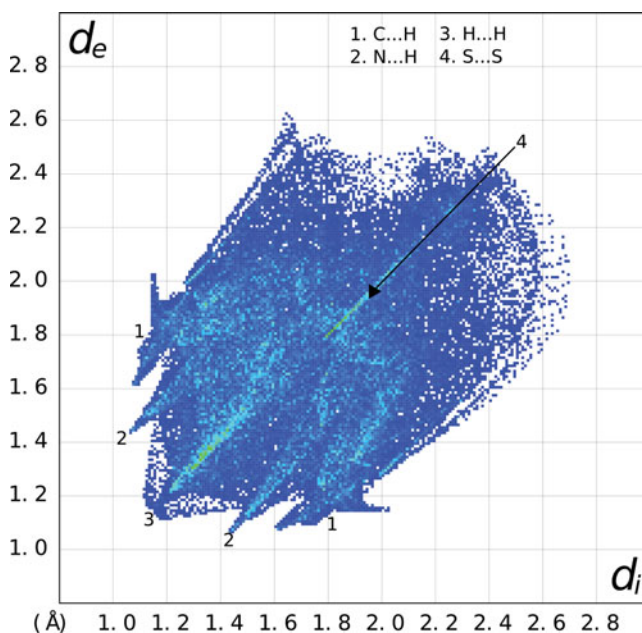


Figure 12. Fingerprint plot of the **3**. Close contacts are divided into four regions; 1 is C...H, 2 is N...H, 3 is H...H, and 4 is S...S. d_i is the closest distance from a given point on the Hirshfeld surface and d_e is the closest external contacts.

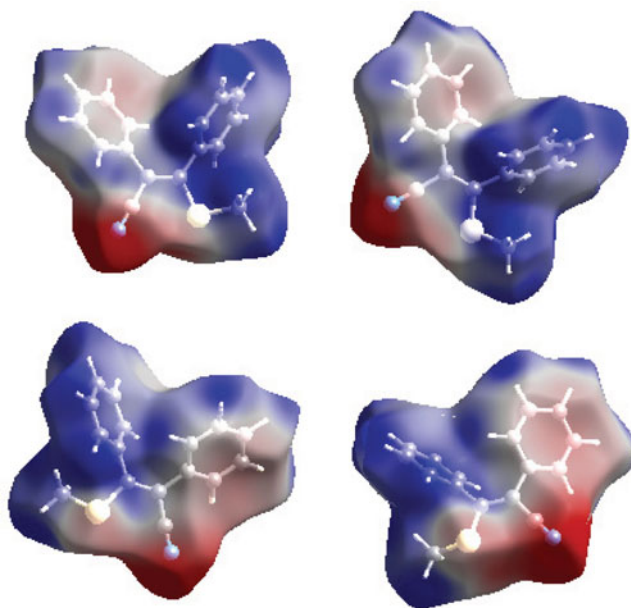


Figure 13. Electrostatic potential mapped on Hirshfeld surface (different orientation) with ± 0.025 au. Blue region corresponds to positive electrostatic potential and red region to negative electrostatic potential.

of the unsaturated connecting units. But the bond length of the atoms S17—C10 (1.755(17) Å) and S17—C18 (1.799(2) Å) have usual values [28]. We observed the deviation of bond angle of $103.47(8)^\circ$ for the atoms C10-S17-C18, from ideal tetrahedral angle, which is due to two nonbonded pairs of electrons over sulfur [29]. The molecule is stabilized by C—H... π interactions confirmed by its distance of 3.6501(18) Å from atom C12 to ring 1, where the C12 acts as a donor and the ring (1) as an acceptor. Fig. 9 represents trifurcated C—H...N hydrogen bonds. The intermolecular hydrogen bond is given in Table 5. Also, there is a weak S...S intermolecular interaction between sulfur atoms with the distance 3.5791(6) Å suggesting electropositivity of the sulfur. This weak intermolecular interaction plays a significant role in the stabilization of crystal structure. The molecule exhibits supramolecular structure, which can be observed from the packing diagram down the *c* axis, as shown in the Fig. 8. In addition to the above, compound **3**, reveals the interaction of the type C—H...N \equiv C, and belongs to supramolecular synthon [30].

3.8. Hirshfeld Surface Analysis

In addition to the structural investigation of the title compound **3**, the intermolecular interactions in the crystal structure are quantified using Hirshfeld surface analysis [31–34]. Hirshfeld surface approach is a graphical tool for visualization and understanding of intermolecular interactions [35, 36]. The compound **3** exhibits intermolecular interactions of the type S...S, C—H... π , and C—N...H. In addition to this, it is constituted with H...H and other intermolecular contacts. Here, we estimate the intermolecular contacts, which are shown in Fig. 10. The chart indicates that the contribution of S...S contact is 2%, which is very less compared to the contribution from other intermolecular contacts N...H (14.7%),

C... H (27.4%), and H... H (47.0%). The contacts C... H, N... H, and S... S contacts are highlighted by conventional mapping of d_{norm} on molecular Hirshfeld surfaces as shown in Fig. 11. This figure shows three orientation of the Hirshfeld surface, where the major contacts (C... H, N... H) are indicated by the dark red spots (figures a, b, and c) and pale red spot (bottom of the figure b) indicate the weak S... S contacts. The intercontacts of the molecule **3** are established using fingerprint plot of Fig. 12. The contacts C... H (label 1: Fig. 12) exhibit the characteristic wings, indicating the presence of C-H... π interactions. H... H (label 3: Fig. 12) contacts are located at the far region on the finger plot. N... H and S... S contacts are represented by label 2 and label 4 (Fig. 12), respectively. The calculated volume inside the Hirshfeld surface is 324.24 Å³. And electrostatic potential is mapped on Hirshfeld surface using STO-3G basis set at the Hartree–Fock theory over the range of ± 0.025 au (Fig. 13). Surface calculation is performed with the TONTO [37] integrated with Crystal explorer [34] using crystal geometries. The positive electrostatic potential (Blue region) over the surface indicates hydrogen donor potential, and hydrogen bond acceptors are represented by negative electrostatic potential (Red region) [38].

4. Conclusion

The title compound (**3**) was synthesized and characterized by ¹H NMR, MS, IR, TGA, and DSC data. The molecular structure of this compound was determined by single crystal XRD method. The intermolecular interactions of the type C–H... π , C–H... N, and S... S connect the molecules exhibiting three-dimensional architecture. In addition, the inter contacts were analyzed using Hirshfeld surfaces analysis.

Acknowledgments

The author M.P.S. thanks Vision Group on Science and Technology, Government of Karnataka No. VGST/SMYSR/2012-13/286 and A.C.V. thanks Council of Scientific and Industrial Research (CSIR, New Delhi) 9/119(0189)2KR-EMR-I for SRF.

References

- [1] Dieter, S., Michael, K., & Bengt, T. G. (1973). Umsetzung metallierter trimethylsilylformaldehyde-thioacetale mit carbonylverbindungen. Eine einfache method grober anwendungsbreitezur herstellung von keten-thioacetalen. *Chem. Berichte.*, 106(7), 2277–2290.
- [2] Carey, F. A., & Neegard, J. R. (1971). Reactions of Ketene thioacetals with electrophiles. A method for homologation of aldehydes. *J. Org. Chem.*, 36(19), 2731–2735.
- [3] Seebach, D., Kolb, M., & Grobel, B. T. (1974). Homologative transformation of aldehydes and ketones to α,β -unsaturated ketones through metalated ketene thioacetals. *Tetrahedron Lett.*, 36(15), 3171–3174.
- [4] Theodore, C., & James, R. M. (1979). Stereochemistry and mechanism of the base-induced loss of thiophenol from 1, 1, 3-tris (phenylthio)alkanes to form cyclopropanone dithioketals. *J. Org. Chem.*, 44(26), 4816–4818.
- [5] Theodlore, C., Robert, B. W., & Richard, E. G. (1979). On the stereochemical aspects of the intramolecular 1, 1-cycloaddition reaction of nitrilimines. *J. Org. Chem.*, 44(25), 4744–4746.
- [6] Francis, A. C., & Court, A. S. (1972). Cycloaddition reactions of vinylketene thioacetals. *J. Org. Chem.*, 37(26), 4474–4476.
- [7] Dieter, S., & Rainer B. D. C. (1975). Micheal additions of metalated thioacetals to cyclic enones. *Angew. Chem. Int. Edit.*, 14(1), 57–58.

- [8] Richard, A. C., & John, Y. L. C. (1982). The ketene thioacetal group as a cationic cyclization terminator. : A synthesis of the pyrrolizidine ring system. *Tetrahedron Lett.*, 23(26), 2619–2622.
- [9] Prabal, P. S., Yadav, A. K., Ila, H., & Junjappa, H. (2009). Novel Route to 2,3-substituted benzo[b]thiophenes via intramolecular radical cyclization. *J. Org. Chem.*, 74(15), 5496–5501.
- [10] Syam Kumar, U. K., Yadav, A. K., Venkatesh, C., Ila, H., & Junjappa, H. (2004). Heteroaromatic annulation studies on 2-[bis(methylthio)methylene]-1-methyl-3-oxoindole: synthesis of novel heterocyclo[b] fused indoles. *Arkivoc.*, (viii), 20–27.
- [11] Nicholas, J. H., John, G. J., Deborah, E. B., Robert, W. D., Harry, M. G., et al. (1992). 3[4-[1-(6-Fluorobenzo[b]thiophen-3-yl)-4-piperazinyl]butyl]-2,5,5-trimethyl-4-thiazolidinone: a new typical antipsychotic agent for the treatment of schizophrenia. *J. Med. Chem.*, 35(14), 2712–2715.
- [12] Javier, M. E., Oficialdegui, A. M., Silvia, P. S., Begona, H., Lara, O., et al. (2001). New 1-aryl-3-(4-arylpiperazin-1-yl)propane derivatives, with dual action at 5-HT_{1A} serotonin receptors and serotonin transporter, as a new class of antidepressants. *J. Med. Chem.*, 44(3), 418–428.
- [13] Guillaume, D. N., Christine, L. A., Alain, R., Marie, O. V., & Tony, J. V. (2003). New fibrinolytic agents: benzothiophene derivatives as inhibitors of the t-PA–PAI-1 complex formation. *Biorg. Med. Chem. Lett.*, 13(10), 1705–1708.
- [14] Hidekazu, M., Yusuke, M., Akira, T., Akira, M., Yuuki, K., et al. Structure–Activity relationship of benzo[b]thiophene-2-sulfonamide derivatives as novel human chymase inhibitors. *Biorg. Med. Chem. Lett.*, 13(22), 4085–4088.
- [15] Diane, H. B., James, B. K., Sonya, S. K., Roderick, J. S., David, T. C. R., et al. Inhibition of E-Selectin-, ICAM-1-, and VCAM-1-mediated cell adhesion by benzo[b]thiophene-, benzofuran-, indole-, and naphthalene-2-carboxamides: identification of PD 144795 as an Antiinflammatory Agent. *J. Med. Chem.*, 38(22), 4597–4614.
- [16] Hong, W. Y., & Daniel, R. A. (1997). highly diastereoselective, tandem mukaiyama aldol-lactonization route to β -lactones: application to a concise synthesis of the potent pancreatic lipase inhibitor, (–)-Panclicin D. *J. Org. Chem.*, 62(1), 4–5.
- [17] Hatwar, R. V., Manivel, P., Khan, F. N., & Row, T. N. G. (2009). Evaluation of intermolecular interactions in thioisocoumarin derivatives: the role of the sulfur atom in generating packing motifs. *Cryst. Eng. Comm.*, 11, 284–291.
- [18] Desiraju, G. R. (2001). Crystal engineering: Outlook and prospectus. *Curr. Sci.*, 81, 1038.
- [19] Kisserwan, H., & Gaddar, T. H. (2010) Enhancement of photovoltaic performance of a novel dye, “T18”, with ketene thioacetal groups as electron donors for high efficiency dye-sensitized solar cells. *Inorg. Chim. Acta.*, 363, 2409–2415.
- [20] Agilent Technologies, CrysAlis PRO Software system, version 1.171.36.2, Agilent Technologies UK Ltd, Oxford, UK; 2011.
- [21] Clark, R. C., & Reid, J. S. The analytical calculation of absorption in multifaceted crystals. *Acta Crystallogr.*, A51, 887.
- [22] Sheldrick, G. M. (1997). SHELXS-97 Crystal Structure Solution, Institute Anog. Chemie, University of Gottingen, Germany.
- [23] Sheldrick, G. M. (1997). SHELXL-97 Program for Crystal Structure Refinement, Institute Anog. Chemie University of Gottingen, Germany
- [24] Macrae, C. F., Edgington, P. R., McCabe, P., Pidcock, E., Shields, G. P., et al. (2006). Mercury: visualization and analysis of crystal structures. *J. Appl. Crystallogr.*, 39, 453–457.
- [25] Meng, X. G., & Wu, A. (2005). Ethyl 2, 5-diphenylfuran-3-carboxylate. *Acta Crystallogr.*, E61, o2808.
- [26] Khalaji, A. D., & Harrison, W. T. A. Crystal structure of β -Phenylcinnamaldehyde-4-bromoaniline. *Anal. Sci.: X-ray Struct. Anal. Online.*, 24, x3–x4.
- [27] Spek, A. L. (1990). PLATON, An integrated tool for the analysis of the results of a single crystal structure determination. *Acta Crystallogr.* A46, C34.
- [28] Nirmala, J., Unnikrishnan, N. V., Ashokan, C. V., Anabha, E. R., & Sudarsanakumar, C. (2008). 2-[2-(4-methylbenzoyl)-3,3-bis(methylsulfonyl)prop-2-enylidene]malononitrile. *Acta Crystallogr.* E64, o592.

- [29] Karmakar, S., Patowary, K., Bhattacharjee, S. K., Deka, B., & Chakraborty, A. (2009). Crystal and molecular structure of 2-thiobenzylazobenzene. *Indian J. Pure Appl. Phys.*, *47*, 863–866.
- [30] Desiraju, G. R., Vittal, J. V., & Ramanan, A. (2011). *Crystal Engineering*, World Scientific Publishing Co Pte. Ltd. 5 Toh Tuck Link, Singapore; 59.
- [31] McKinnon, J. J., Spackman, M. A., & Mitchell, A. S. (2004). Novel tools for visualizing and exploring intermolecular interactions in molecular crystals. *Acta Crystallogr. B60*, 627–668.
- [32] Spackman, M. A., & Jayatilaka, D. (2009). Hirshfeld surface analysis. *Cryst. Engg. Comm.*, *11*, 19–32.
- [33] Spackman, M. A., & McKinnon, J. J. (2002). Fingerprinting intermolecular interactions in molecular crystals. *Cryst. Engg. Comm.*, *4*, 378–392.
- [34] Wolff, S. K., Grimwood, D. J., McKinnon, J. J., Jayatilaka, D., Spackman, M. A. (2007). Crystal Explorer 2.1 University of Western Australia, Perth, Australia.
- [35] McKinnon, J. J., Jayatilaka, D., & Spackman, M. A. (2007). Towards quantitative analysis of intermolecular interactions with Hirshfeld surfaces. *Chem. Commun.*, 3814–3816.
- [36] Munshi, P., Jelsch, C., Hathwar, V. R., & Row, T. N. G. (2010). Experimental and theoretical charge density analysis of polymorphic structures: case of coumarin 314 dye. *Cryst. Growth. Des.*, *10*, 1516–1526.
- [37] Jayatilaka, D., Grimwood, D. J., Lee, A., Lemay, A., Russell, A. J., et al. (2006). TONTO - A system for computational chemistry.
- [38] Spackman, M. A., McKinnon, J. J., & Jayatilaka, D. (2008). Electrostatic potentials mapped on Hirshfeld surfaces provide direct insight into intermolecular interactions in crystals. *Cryst. Engg. Comm.*, *10*, 377–388.